This article has been accepted for publication in a future issue of this journal, but has not been fully edited. Content may change prior to final publication. Citation information: DOI 10.1109/JETCAS.2021.3049788, IEEE Journal on Emerging and Selected Topics in Circuits and Systems

A Completely Distributed Economic Dispatching Strategy Considering Capacity Constraints

Hua Han, Xinyu Chen, Zhangjie Liu, Yonglu Liu, Mei Su, Shimiao Chen

***Abstract*—For islanded microgrids integrating distributed generators (DGs) with different generation cost and capacity, economic dispatch (ED) is its one of the key performance attributes and challenges. This paper proposes a completely distributed control strategy with improved reliability, flexibility and voltage quality for DC microgrids. Only depending on a sparse communication graph and neighbor information, the output power of each DG is adjusted to obtain global economic optimization while meeting the load demands and its capacity constraint by switching its control mode between distributed dispatch based on dynamic consensus algorithm and constant power control smoothly. The bus voltage is recovered accurately by construct a shortest communication line between bus agent and one DG to obtain the bus voltage. The stability and convergence of the proposed scheme have been analyzed. Simulation test has verified the feasibility and validity of the proposed control strategy.**

***Index Terms*—Distributed control, cost optimization, capacity constraints, DC microgrids**

I. Introduction

A. Motivation and Incitement

Recently, interest has been concentrated on microgrids [1]-[4], which is the most effective way to solve the penetration of extensively distributed generators (DGs) to power grid [5, 6]. Compared with AC microgrids, DC microgrids don't involve frequency deterioration, reactive power compensation, and multi-stage power conversion, which helps to increase the capacity of transmission line and improve the reliability of power supply and reduce system loss [7].

Economical dispatch (ED) is considered as one of the core problems in microgrid research. Usually, a microgrid consists of different types of DGs that have different generation costs [8, 9]. From the perspective of economics, all DGs should be dispatched within their capacity constraints to minimize the generation cost of system and system exhibits high voltage quality, robustness, stability and communication reliability. The research of ED has been more popular on DC microgrid.

Manuscript received September 30, 2020; revised December 5, 2020 and December 26, 2020; accepted January 3, 2021. This work was supported in part by the National Natural Science Foundation of China under Grant 61933011 and 61903383, Hunan Provincial Key Laboratory of Power Electronics Equipment and Grid under Grant 2018TP1001, the Fundamental Research Funds for the Central Universities of Central South University under Grant 2020zzts581, and Hunan Province Strategic Emerging Industry Science and Technology Research and Major Scientific and Technological Achievements Transformation Project 2018GK4016. (Corresponding author: Zhangjie Liu.)

H. Han, X Chen, Z. Liu, Y. Liu, M. Su and S. Chen are with the school of Automation, Central South University and the Hunan Provincial key Laboratory of Power Electronics Equipment and Gird, Changsha 410083, China(e-mail: hua_han@126.com, 194612109@csu.edu.cn, zhangjieliu@csu.edu.cn, liuyonglu@csu.edu.cn, sumeicsu@csu.edu.cn, shimiaochen@csu.edu.cn).

B. Literature Review

The method to solve the ED can be divided into decentralized algorithm, centralized algorithm and distributed algorithm according to the degree of dependence on communication. Owing to the high reliability and communication-free features, decentralized economical operation schemes represented by the droop control have drawn plenty of research studies [10]. However, the global optimum is not guaranteed and there is a voltage deviation, due to relying on no communication infrastructure [11]-[12]. Various centralized algorithms have been proposed to solve ED. In [11], a lambda iteration approach was proposed. Intelligent optimization algorithms, such as particle swarm optimization and genetic algorithm [13]-[17] are also developed to solve the ED with inequality constraints in recent years. [16] proposes a general framework which can be applied to any evolutionary algorithm for handling constraints in ED problems. In [17], an improved binary artificial fish swarm algorithm (IBAFSA) and a fast constraint processing mechanism are presented to solve the large-scale unit commitment problems of large-scale power systems, which handles the coupling between system spinning reserve constraint and unit minimum up and down time constraint. However, centralized methods have the disadvantages of single-point failure, high communication requirements and poor scalability.

Distributed control has been developed to take place of the decentralized control and centralized control with good reliability and simple communication network requirement [18]-[21]. [18] proved that distributed control is still effective considering communication delays and slow switching topologies. [19] provides a theoretical analysis tool for communication delay and load uncertainty. distributed control can be applied in noisy environments by employing event-triggered communication mechanism. [20] proved that the amount of communication can be minimized in a distributed system by employing event-triggered communication mechanism in noisy environments. Besides, [21] offers a valid nonlinear distributed cooperative control scheme in a sparse cyber network subject to noisy disturbance and limited bandwidth constraints.

Because the distributed system has high control accuracy and low communication dependence, global optimal ED can be achieved in a distributed manner. [22]-[24] presented a series of distributed control methods based on adaptive virtual impedance to achieve optimal power dispatch and properly load sharing by synchronizing incremental costs of all DGs. The author in [25] proposes a continuous-time distributed optimal control for DC micro-grids system with communication delays, which can effectively solve the problem of economic

This article has been accepted for publication in a future issue of this journal, but has not been fully edited. Content may change prior to final publication. Citation information: DOI 10.1109/JETCAS.2021.3049788, IEEE Journal on Emerging and Selected Topics in Circuits and Systems

TABLE I
MERITS AND GAPS OF EXISTING METHODS

Current method	Advantages	Disadvantages
Project algorithm [26]	Good scalability and supporting plug-and-play	Lack of voltage recovery
"Virtual ICR" [27]-[30]	Global optimal ED in discrete consensus	Not global optimal ED in dynamic consensus
Method with GLO [31]	Global optimal ED in dynamic consensus	Lack of plug-and-play
Average voltage recovery [25],[31]	Partly voltage recovery	Low accuracy of recovery
Voltage recovery by line impedance [32]	Higher accuracy of voltage recovery	Low robustness

dispatch, but it doesn't consider the capacity constraints of DGs and the quality of voltage need to be improved. However, the above method solving the global optimal ED don't take capacity constraint into account. Therefore, several studies are developed to deal with capacity constraints. [26] proposes a projected algorithm with good scalability to solve the capacity constraint, but this method does not consider voltage recovery and the reliability of system power supply need to be improved. "virtual ICR" is presented to solve the ED with capacity constraint based on discrete consensus algorithm [27]-[30], but it can't realize global optimal ED in dynamic consensus. A global load observer (GLO) is introduced to realize ED with consideration of capacity constraints [31]. However this method demands that every DG need know coefficients of cost function of all DGs in advance and plug-and-play can't be achieved. Although average voltage recovery is adopted in [25] [31] when considering capacity constraint in ED, the accuracy of voltage recovery still need to be improved. In [32], the author realizes higher accuracy of bus voltage recovery by estimating impedance information. If there is an estimation error in the line impedance, the voltage cannot be restored accurately, so the robustness of this method is low.

The merits and gaps of existing distributed method are summarized in Table I. To the best of our knowledge, there is no distributed strategy considering capacity constraint in ED satisfying requirements to global economic optimization, high voltage quality and robustness (such as plug-and-play, time-varying delay and communication noise) simultaneously.

C. Contribution and Paper Organization

Motivated by the above considerations, we further propose a distributed ED algorithm considering capacity constraint, which exhibits high voltage quality, robustness and communication reliability. The contributions of this paper are summarized as following:

- Global optimal ED considering capacity constraint: a novel completely distributed ED scheme is presented without load observers. This ED scheme consists of distributed coordinate control base on dynamic consensus and constant power control, the control mode switching of each DG is triggered by its output power. The DGs operate in constant power mode when their output powers reach the capacity bounds, otherwise, they are dispatched by dynamic consensus algorithm to reach global economic optimization. The proposed method can adjust the output power of all DGs within their capacity constraints to response the change of load in real time.
- Voltage recovery: Based on the communication between one DG and bus agent, a voltage recovery mechanism is proposed. One of DGs undertakes voltage recovery whether its output power is limited or not. Compared with average voltage recovery method [25] [31] and voltage recovery based on line impedance estimation [32], this proposed method can achieve high voltage quality only relying on the voltage of bus transmitted to one of DGs, which improve the reliability and voltage quality of system.
- Good robust performance: plug-and-play can be achieved in the proposed method. Besides, our method can resist certain communication delay, noise disturbances and load change. The effect of communication delay and load change are analyzed in theory.

The remainder of the paper is organized as follows. Section II formulates the model of economic dispatching in DC microgrid and related studies, which aims to minimize the generation cost and meet power balance and capacity constraints. In Section III, a completely distributed economic dispatching strategy is proposed to solve the problem in the Section II. Section IV analyzes the convergence and stability of the proposed method. Case studies are given in Section V to test the proposed method. Finally, Section VI concludes the whole paper.

II. PROBLEM FORMULATION

A. ED Within Capacity Constraint

The configuration of DC microgrid is shown in Fig.1(a). There are conventional generators (CGs) such as diesel generators and micro-turbines, renewable generators (RDGs) such as photovoltaic systems (PVs) and wind turbines (WTs), energy storage units (ESUs) and loads.CGs and ESUs are dispatchable distributed generators (PDGs). RDGs are not dispatchable and operate at maximum power point (MPP).

The cost function of PDG is commonly defined as quadratic polynomials,

$$C_i(p_i) = \gamma_i p_i^2 + \beta_i p_i + \alpha_i \tag{1}$$

where $C_i(p_i)$ is the generation cost of PDG$_i$, p_i is the output active power of PDG$_i$, γ_i, β_i, α_i are the constant coefficients of cost function of PDG$_i$.

The goal of ED is to minimize the generation cost considering capacity constraints of PDGs, the problem can be formulized as

$$\begin{cases} \min \sum_{i=1}^{n} C_i(p_i) \\ \sum_{i=1}^{n} p_i = p_{load} - p_{loss} \\ 0 \le p_i \le p_i^{\max} \end{cases} \tag{2}$$

This article has been accepted for publication in a future issue of this journal, but has not been fully edited. Content may change prior to final publication. Citation information: DOI 10.1109/JETCAS.2021.3049788, IEEE Journal on Emerging and Selected Topics in Circuits and Systems

where p_{load} is the total load power, p_{loss} is the power loss in power transmission, $p_i^{\max}$ is the maximum output power of PDG$_i$, n denotes the number of PDGs.

The augmented Lagrange function of (2) is given by

$$L(p_1, p_2, \cdots, p_n, \lambda) = \sum_{i=1}^{n} C_i(p_i) - \lambda(\sum_{i=1}^{n} p_i - p_{load} + p_{loss}) \tag{3}$$

where λ is the Lagrange multiplier. Because the objective function is smooth and convex, then the solution to the ED described by (3) is achieved.

$$\begin{cases} \frac{\partial L}{\partial p_i} = 2\gamma_i p_i + \beta_i - \lambda = 0 \\ \frac{\partial L}{\partial \lambda} = \sum\limits_{i=1}^{n} p_i - p_{loss} - p_{load} = 0 \end{cases} \tag{4}$$

λ_i is assumed as the incremental cost rate (ICR) of PDG$_i$. The global optimal solution of (4) is determined by (5)

$$\lambda_1 = \lambda_2 = \cdots = \lambda_n \tag{5}$$

To achieve (5), a fast distributed gradient method based on equal ICR criteria is proposed [33]. Moreover, the author in [34] adopts a proposed method by combining ICRs from its neighbors to solve ED. Without considering the capacity constraint, the above methods can effectively solve ED.

B. ED With Capacity Constraint

The actual ED problem must take capacity constraint into consideration. In general, the current methods for ED capacity constraint are mainly divided into two groups. The first group is discrete consensus. In [27]-[30], the author adopts "virtual ICR" to solve the problem of capacity constraint. When the DG reaches the limit value, its output power remains constant, but the ICR of the bound DG continue to participate in other ICRs' update. The global optimal ED can't be guaranteed.

The other group is dynamic consensus, shown as (6)

$$\begin{cases} \lambda_i(k+1) = 2\gamma_i p_i(k) + \beta_i \\ u^* = u_{ref} + \sum\limits_{j \in N_i} a_{ij}\left(\lambda_j(k+1) - \lambda_i(k+1)\right) + \delta u \end{cases} \tag{6}$$

where δu is the bus voltage compensation item. As for dynamic consensus, it is inappropriate to use the method of "virtual ICR", because the ICR of the bound DG is constant and the result of the last outcome is not optimal, because the ICR in dynamic consensus is calculated by the output power. Besides, if forcing the ICR of the bound DG to exit the iteration, the system also wil not reach the lower cost because the structure of communication is no longer a spinning tree. In [31], a load observer is used to estimate the total load to judge whether the output powers of PDGs reach their limitation of capacities. However, the scale of DC microgrid system based on this ED method is limited, and the performance of plug and play is lost.

In view of the above problems, this paper proposes a novel dynamic consensus based distributed ED scheme to improve system economy, flexbility, relaibility and stability without load observer.

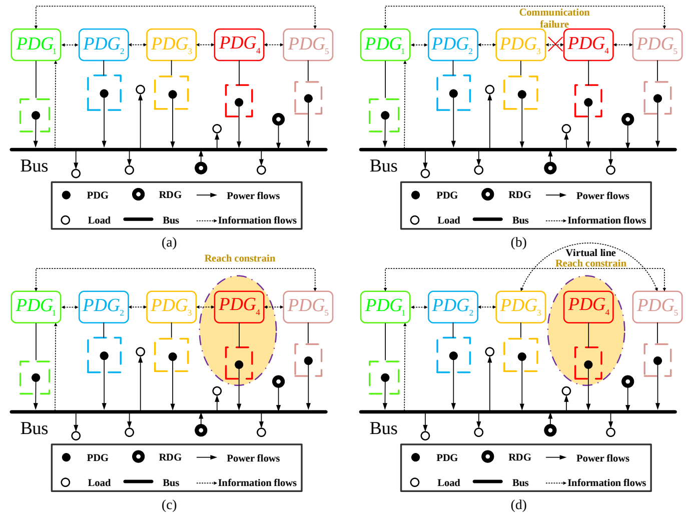

Fig. 1. Block diagram of DC micro-grid. (a) Cyber-physical system, (b) Communication failure, (c) Reach constrain, (d) Constrain equivalent graph

III. THE PROPOSED DISTRIBUTED ED SCHEME

DC microgrid can be seen as a cyber-physical system with a communication network facilitating information exchange among PDGs for control purpose. To achieve ED and high voltage quality of DC microgrid with capacity constraints, a distributed ED scheme is presented to adjust the output power of each PDG by smooth switching between lambda dynamic consensus mode and constant power mode.

A. The Communication Topology

In order to facilitate both distributed ED and voltage recovery of islanded DC micro-grid including n PDG, a low bandwidth communication network shown in Fig.1 is designed. The communication graph consists of $n+1$ nodes $V_G = \{\nu_0, \nu_1, \cdot \cdot \cdot, \nu_n\}$ connected via a set of edges. In subgraph $V_{G1} = \{\nu_1, \nu_2, \cdot \cdot \cdot, \nu_n\}$, communication links are bidirectional to form an undirected graph, and each node only exchanges information with nodes represented by N_i next to it. N_i denotes the set of all neighbors of node ν_i. When some communication line fails, there is still a spinning tree to keep a communication path including all the PDGs in V_{G1} as shown in Fig.1(b), and both the sparsity and reliability of communication network is ensured. In addition, a special unidirectional link between ν_0 to ν_1 is set, thus the bus voltage information can be transmitted from node ν_0 to node ν_1 to restore the bus voltage.

The sub communication graph V_{G1} is represented by an associated adjacency matrix $A_{G1} = [a_{ij}] \in R^{n \times n}$, where $a_{ij} = 1$ if there are an edge connecting node v_i to node v_j, and $a_{ij} = 0$, otherwise. The Laplacian matrix of communication subgraph V_{G1} is $L = diag\{d_i^{\text{in}}\} - A_{G1}$, where $d_i^{\text{in}} = \sum\limits_{j \in N_i} a_{ij}$.

B. Economic Dispatch Considering Capacity Constraints

The proposed distributed control architecture takes each PDG as an intelligent agent, and each agent only exchanges information with its neighbor agents to obtain real-time economic dispatch.

This article has been accepted for publication in a future issue of this journal, but has not been fully edited. Content may change prior to final publication. Citation information: DOI 10.1109/JETCAS.2021.3049788, IEEE Journal on Emerging and Selected Topics in Circuits and Systems

1) Output power within constraint: The objective of economic dispatch of system is to adjust the output power of each PDG within its power constraint, in order to control the ICRs of all PDGs to the same value in a distributed manner. The distributed control strategy is described as follows:

$$\begin{cases} u_i^* = u_{ref} - r_{vir} i_i + \delta u_i^1 \\ \delta u_i^1 = k_\lambda \int \sum\limits_{j \in N_i} a_{ij} (\lambda_{j\_i} - \lambda_i) dt \quad (i > 1) \\ 0 < p_i < p_i^{\max} \end{cases} \tag{7}$$

where u_{ref} is the rated voltage, u_i^* is the expected output voltage of PDG$_i$, i_i is the output current of PDG$_i$, u_{pcc} is the bus voltage, p_i and $p_i^{\max}$ are the output power and maximum output power of PDG$_i$, respectively. r_{vir} is the virtual impedance, which plays a damping and improving the stability of system role, δu_i^1 denotes ED compensation of PDG$_i$, k_λ denotes integral coefficient. $\lambda_{j\_i}(t)$ is the information broadcast from PDG$_j$ to PDG$_i$.

2) Output power being limited: When the output power of PDG$_i$ has reached maximum, the control strategy described by (7) must be modified because PDG$_i$ should keep constant power output, shown as (8)

$$\begin{cases} u_i^* = u_{ref} - r_{vir} i_i + \delta u_i^2 \\ \delta u_i^2 = k_p \int (p_i^{\max} - p_i) \mathrm{d}t \quad (i > 1) \\ p_i \geq p_i^{\max} \end{cases} \tag{8}$$

where δu_i^2 denotes maximum power compensation of PDG$_i$, k_p denotes integral coefficient.

C. Voltage Adjust Considering Capacity Constraints

In order to realize bus voltage recovery, an intelligent agent is designed to receive the value of bus voltage and undertake voltage recovery. Assume that PDG$_1$ is nearest to the bus and undertake the task of bus voltage regulation, whose control strategy is different from other PDGs.

1) Output power within Capacity constraints: When PDG$_1$ is within capacity constraint, the control strategy is described as follows:

$$\begin{cases} u_i^* = u_{ref} - r_{vir} i_i + \delta u_i^3 \\ \delta u_i^3 = k_u \int (u_{ref} - u_{pcc}) \, dt \quad (i = 1) \\ 0 < p_i(t) < p_i^{\max} \end{cases} \tag{9}$$

where δu_i^3 represent voltage recovery compensation of PDG$_i$. k_u denotes integral coefficient. u_{pcc} is the voltage of DC bus.

2) Output power being limited: When the output power of PDG$_1$ reaches maximum, its control strategy switches from (9) to (10)

$$\begin{cases} u_i^* = u_{ref} - r_{vir} i_i + \delta u_i^2 \\ \delta u_i^2 = k_p \int (p_i^{\max} - p_i) \mathrm{d}t \quad (i = 1) \\ p_i \geq p_i^{\max} \end{cases} \tag{10}$$

It is noted that voltage recovery compensation is delivered from PDG$_1$ to other PDGs, which will be explained in the following section.

D. Communication Transmission and Detection Protocol

To ensure ED can be achieved during the entire operation, different PDG will have different control strategy and different communication transmission protocol. Meanwhile the goal of detection protocol is to guarantee the accuracy of the switching control strategy.

1) Communication Transmission Protocol: As for PDG$_i$ whose output power is within the constraint, the information transmitted from it to its neighbor PDG$_j$ is

$$\lambda_{i\_j} = \lambda_i \tag{11}$$

When PDG$_1$ is controlled in maximum power output mode, the information will be changed to

$$\lambda_{1\_j} = \lambda_1 + \delta u_1^3 \tag{12}$$

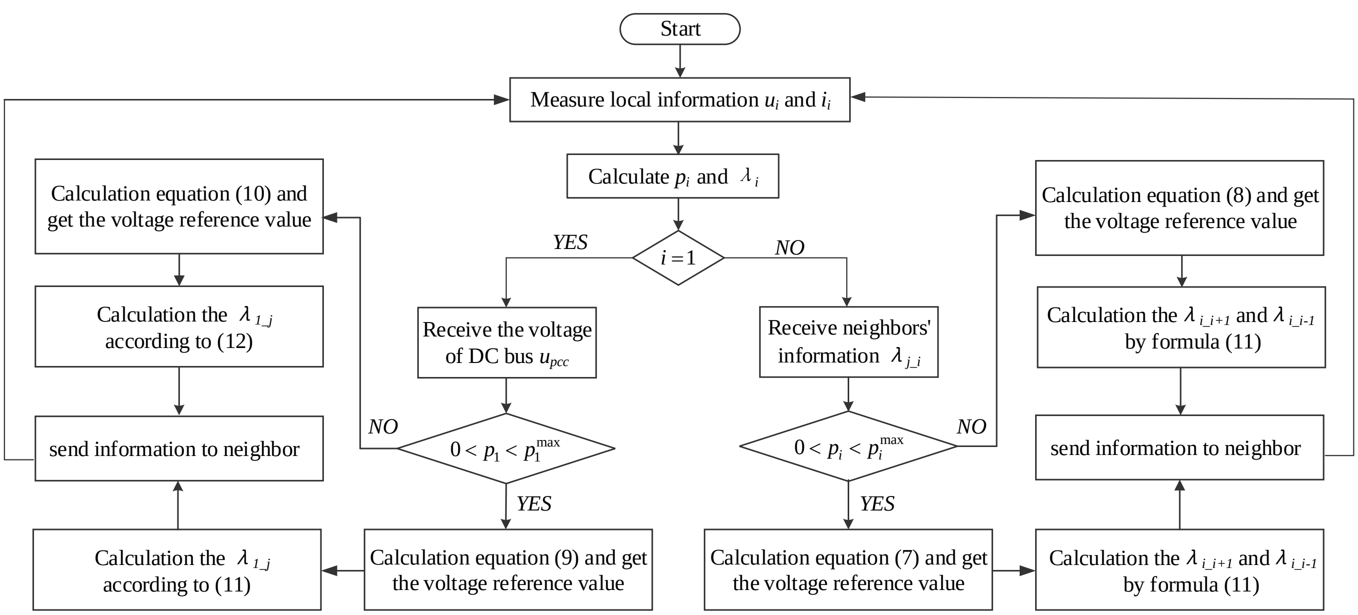

Fig. 2. Schematic diagram of control flow

This article has been accepted for publication in a future issue of this journal, but has not been fully edited. Content may change prior to final publication. Citation information: DOI 10.1109/JETCAS.2021.3049788, IEEE Journal on Emerging and Selected Topics in Circuits and Systems

By (12), the task of voltage recovery is passed to other PDG.

As for $\mathrm{PDG}_i (i > 1)$, when its output power reaches the capacity constraint, the information to its neighbor are

$$\begin{cases} \lambda_{i\_i-1} = \lambda_{i+1\_i} = \lambda_{i+1} \\ \lambda_{i\_i+1} = \lambda_{i-1\_i}{=}\lambda_{i-1} \end{cases} (i > 1) \tag{13}$$

Subscript $i-1, i+1$ denote different neighbor of $\mathrm{PDG}_i(i > 1)$,$N_i = \{v_{i-1}, v_{i+1}\}$. Equation (13) shows that the bound PDG becomes a virtual communication line between its neighbors, as shown Fig.1(d).

2) Detection Protocol: How PDG switches its control strategy smoothly and precisely is important. In this paper, a valid method is proposed to make sure PDGs adjust their own control mode adaptively.

When PDG has not reach the constraint, it compares its output power with the maximum power regularly. The detection time interval depends on the performance of the control equipment. As long as the output power has exceeds the maximum power in two consecutive detections, the PDG will switch to maximum output power mode automatically. And then, when the output of PDG maintains maximum power, it compares its own λ with $\bar{\lambda}$, $\bar{\lambda}$ is the mean value of neighbors' λ. The condition that the PDG switches to dynamic dispatch mode from maximum power output mode is $\bar{\lambda}$ is less than λ in two consecutive detections.

$$\bar{\lambda}{=}\frac{\sum\limits_{j\in N_i}\lambda_j}{\sum\limits_{j\in N_i} a_{ij}} \tag{14}$$

E. Global Control Strategy

The overall flow chart and control structure are shown in Fig.2 and Fig.3, respectively. When the output of each PDG is within power constraint, the following equation deduced from (11)

$$\sum_{j\in N_i} a_{ij}(\lambda_{j\_i} - \lambda_i) = \sum_{j\in N_i} a_{ij}(\lambda_j - \lambda_i) = \sum_{j\in N_i} a_{ij}\lambda_j - d_i^{in}\lambda_i \tag{15}$$

The sub communication graph VG_1 is a Laplacian matrix. Accordingly, one can formulate the global dynamic in the complex frequency domain as

$$\begin{cases} U^* = U_{ref} - r_{vir}I + \delta U^1 + \delta u_1^2\tau \\ \delta U^1 = -\frac{k_\lambda}{s}(I_n - \tau\tau^T)L\Lambda \\ \delta u_1^2 = \frac{k_u}{s}(u_{ref} - u_{pcc}) \end{cases} \tag{16}$$

where $U^* = [u_1^*, \cdots, u_n^*]^T$,$I = [i_1(t), \cdots, i_n(t)]^T$, $\Lambda = [\lambda_1, \cdots, \lambda_n]^T$,$\tau = [1, 0, \cdots, 0]^T$,$U_{ref} = u_{ref}1_n$, $1_n \in R^n$ and $1_n = \begin{bmatrix} 1 & 1 & \cdots & 1 \end{bmatrix}^T$.

When PDG_1 reach the limited value, based on (8) (10) (12), one can formulate the global control strategy

$$\begin{cases} U^* = U_{ref} - r_{vir}I + \delta U^1 + \delta u_1^3\tau \\ \delta U^1 = -\frac{k_\lambda}{s}(I_n - \tau\tau^T)L\left(\Lambda + \delta u_1^2\tau\right) \\ \delta u_1^3 = \frac{k_p}{s}(p_1^{\max} - p_1) \end{cases} \tag{17}$$

In addition, when $\mathrm{PDG}_i(i > 1)$ reaches the constraint, as for other PDGs, the derivation is the same as (16).

IV. STEAD-STATE AND STABILITY ANALYSIS

In this part, the system stability and steady-state performances with the proposed control strategy is studied. The control parameters are properly tuned, which is based on stability analysis. Meanwhile steady-state performance is verified by proof of convergence.

A. All PDGs within Capacity Constraints

Steady-state analysis of the DC microgrid system is essential to ensure that the cooperative controllers satisfy both operational requirements: the bus voltage recovery and the cost optimization.

When all PDGs are within constraint, according to (9), for $t \geq t_0$, one can write

$$u_1^{*^{ss}} = u_{ref} - r_{vir}i_1^{ss} + k_u(u_{ref} - u_{pcc}^{ss})(t - t_0) + W_u(t_0) \tag{18}$$

where x^{ss} denotes the steady-state value of the variable x. $W_u(t_0)$ is a value that carries integrator output of the voltage regulators at $t = t_0$. In steady state, the time-varying term in (18) is zero.

$$k_u(u_{ref} - u_{pcc}^{ss})t = 0 \rightarrow u_{pcc}^{ss} = u_{ref} \tag{19}$$

Similarly, one can write based on (16)

$$(I_N - \tau\tau^T)k_\lambda L\Lambda^{ss} - k_u(u_{ref} - u_{pcc}^{ss})\tau = 0_n \tag{20}$$

where $0_n \in R^n$ and $0_n = \begin{bmatrix} 0 & 0 & \cdots & 0 \end{bmatrix}^T$.

Substituting (19) into (20) yield

$$(I_N - \tau\tau^T)k_\lambda L\Lambda^{ss} = 0_n \tag{21}$$

where $(I_N - \tau\tau^T)$ is a diagonal matrix, k_λ is a constant coefficient. Thus, according to Theorem 1 (see Appendix I),

$$L'\Lambda^{ss} = 0_n \tag{22}$$

where $L' = L(I_N - \tau\tau^T)k_\lambda L$ is a balanced Laplacian matrix, then

$$\Lambda^{ss} = m1_n \tag{23}$$

where m is a positive real number.

Equation (19) and (23) show that both the bus voltage recovery and cost optimization are guaranteed.

B. Output Power of PDG_1 being Limit

When any $\mathrm{PDG}_i(i > 1)$ reaches the constraint, the steady-state analysis for other PDGs is the same as the previous section (see A. All PDGs within Capacity Constraints). So it is only considered the circumstance where PDG_1 reaches the limited value.

Similar to (18) (19), for $t > t_0$, one can get from (10)

$$p_1^{ss} = p_1^{\max} \tag{24}$$

According to (17), we have

$$\begin{aligned} &k_\lambda(I_N - \tau\tau^T)\Big(L(\Lambda^{ss} - k_u t_0(u_{_{ref}} - u_{_{pcc}}^{ss})\tau + W_u(t_0)\tau)\Big) \\ &+ (t - t_0)\left(u_{_{ref}} - u_{_{pcc}}^{ss}\right)k_\lambda k_u(I_N - \tau\tau^T)L\tau + W_\lambda(t_0) \\ &- k_p(p_1^{\max} - p_1)\tau = 0_n \end{aligned} \tag{25}$$

This article has been accepted for publication in a future issue of this journal, but has not been fully edited. Content may change prior to final publication. Citation information: DOI 10.1109/JETCAS.2021.3049788, IEEE Journal on Emerging and Selected Topics in Circuits and Systems

Equation (25) holds for all $t \geq t_0$ and $k_\lambda k_u (I_N - \tau\tau^T) L\tau \neq 0_n$, thus $u_{pcc}^{ss} = u_{ref}$.

Substituting $u_{pcc}^{ss} = u_{ref}$ and $p_1^{ss} = p_1^{\max}$ into (25),

$$k_\lambda \left(I_N - \tau\tau^T\right) \left(L(\Lambda^{ss} + W_u(t_0)\tau)\right) = 0_n \tag{26}$$

Similar to (21)-(22), we obtain

$$\Lambda^{ss} + W_u(t_0)\tau = \tilde{m}1_n \tag{27}$$

it is proved that

$$\tilde{\Lambda}^{ss} = \tilde{m}1_{n-1} \tag{28}$$

where $\tilde{m}$ is a positive real number and $\Lambda^{ss} = \begin{bmatrix} \lambda_1 \\ \tilde{\Lambda}^{ss} \end{bmatrix}$. Equation (28) ensures consensus of the ICR, thus achieving global optimization.

C. Stability Analysis Considering Communication Delay and Change of Load

1) Network Modeling: A definite system including PDGs, resistive loads, and line resistances, can be regarded as an n-port network, where all PDGs and loads are nodes. When the system is in steady state, according to Kirchhoff's voltage and current theorem

$$\begin{bmatrix} I \\ i_{load} \end{bmatrix} = \begin{bmatrix} L_{ss} & L_{sl} \\ L_{ls} & L_{ll} \end{bmatrix} \begin{bmatrix} U \\ u_{load} \end{bmatrix} \tag{29}$$

In Fig.1, multiple loads in parallel can be equivalent to one load, expressed as $y_{load}(t)$, which satisfies

$$\begin{cases} y_{load}(t) = y_{load} + \Delta y_{load}(t), y_{load}(t) \in R \\ |\Delta y_{load}(t)| \leq \xi, \xi > 0 \end{cases}$$

and $L_{ss}, L_{sl}, L_{ls}, L_{ll}$ are constant matrices, which are determined by the line resistance(seen in Appendix II). So i_{load} and u_{load} have the following relationship

$$i_{load} = y_{load}(t) u_{load} \tag{30}$$

$$u_{pcc} = u_{load} = -(y_{load}(t) + L_{ll})^{-1} L_{ls} U \tag{31}$$

According to (29) and (31), we obtain

$$I = YU \tag{32}$$

where $Y = (L_{ss} - L_{sl}(y_{load}(t) + L_{ll})^{-1} L_{ls})$, which denotes admittance matrix and $Y_0 = (L_{ss} - L_{sl}(y_{load} + L_{ll})^{-1} L_{ls})$.

2) Linearization model: The small signal model considering communication delay $d(t)$, can be derived from (4), (16) and (32)

$$\Delta\Lambda = \gamma\Delta P = \gamma\Phi\Delta U \tag{33}$$

$$\begin{cases} \Delta\dot{I} = Y\Delta\dot{U} \\ \Delta u_{pcc} = -(y_{load}(t) + L_{ll})^{-1} L_{ls} \Delta U \end{cases} \tag{34}$$

$$\Delta\dot{U} = -r_{vir}\Delta\dot{I} + \Delta\delta\dot{U}^1(t - d(t)) + \Delta\delta\dot{u}_1^3(t - d(t))\tau \tag{35}$$

where $\Phi = diag\left\{i_i^{ss}\right\} + diag\left\{u_i^{ss}\right\} Y, \gamma = diag\{2\gamma_i\}$ and $d(t)$ is a time-varying differentiable function that satisfies

$$\begin{cases} 0 \leq d(t) \leq c \\ \left|\dot{d}(t)\right| \leq \mu \end{cases} \tag{36}$$

where $c > 0$ and $\mu > 0$ are constants. Based on (33)–(35)

$$\Delta\dot{U} = (I_n + r_{vir}Y)^{-1} T\Delta U(t - d(t)) \tag{37}$$

where $T = k_u(y_{load}(t) + L_{ll})^{-1}\tau L_{ls} - k_\lambda(I_n - \tau\tau^T)L\gamma\Phi$.

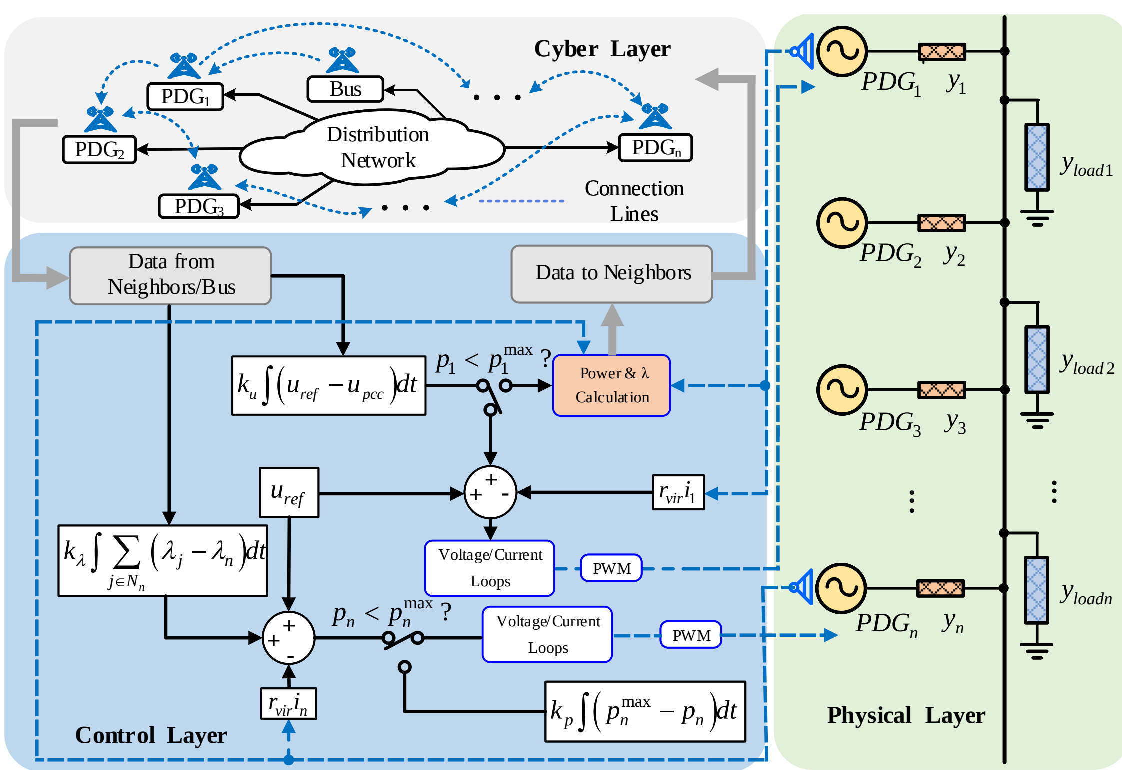

Fig. 3. Block diagram of the proposed control method

This article has been accepted for publication in a future issue of this journal, but has not been fully edited. Content may change prior to final publication. Citation information: DOI 10.1109/JETCAS.2021.3049788, IEEE Journal on Emerging and Selected Topics in Circuits and Systems

When all PDGs are within the constraint, the linearization dynamic model of the entire system considering time-varying structured uncertainties based on (37) is formed as,

$$\dot{X} = (A_{d1} + \Delta A_{d1}(t))X(t - d(t)) \tag{38}$$

where $X = \Delta U$ and $\Delta A_{d1}(t)$ denotes the load change uncertainty. A_{d1} and ΔA_{d1} are given in Appendix III.

Similarly, the small signal model of the system when PDG$_1$ is restricted can be established as

$$\begin{cases} \Delta \dot{U} = -r_{vir}\Delta \dot{I} + \Delta\delta\dot{U}^1(t - d(t)) + \Delta\delta\dot{u}_1^3\tau \\ \Delta\dot{u}_{pcc} = -(y_{load}(t) + L_{ll})^{-1}L_{ls}\Delta\dot{U} \end{cases} \tag{39}$$

(39) can be written as

$$\dot{X} = (A_{b2}+\Delta A_{b2}(t))\, X + (A_{d2} + \Delta A_{d2}(t))\, X(t - d(t)) \tag{40}$$

where $X = \begin{bmatrix} \Delta U \\ \Delta u_{pcc} \end{bmatrix}$, A_{b2}, A_{d2} are shown in Appendix III.

3) Analysis of Time-varying Structured Uncertainties: As for (38) and (40), the uncertainties take following forms

$$\begin{cases} \Delta A_{d1}(t) = F(t)E_{d1} \\ \begin{bmatrix} \Delta A_{b2}(t) & \Delta A_{d2}(t) \end{bmatrix} = F(t)\begin{bmatrix} E_{b2} & E_{d2} \end{bmatrix} \end{cases} \tag{41}$$

E_{d1}, E_{b2} and E_{d2} are given in Appendix III. $F(t) = \Delta y_{load}(t)/\xi$, and $|F(t)| < 1$.

Theorem 2: Given c and μ, if there exists matrices $P = P^T > 0, Q = Q^T \geq 0, R = R^T \geq 0, Z_i = Z_i^T > 0,\ i = 1, 2.$ $N = [N_1, N_2, N_3]^T, S = [S_1, S_2, S_3]^T, M = [M_1, M_2, M_3]^T$ and a scalar $\sigma > 0$, where N, S, and M are freedom matrices that satisfies (42), the system is robustly stable.

$$\begin{bmatrix} \hat{\Psi} & cN & cS & cM & cA_{ci}^T\hat{Z} & \hat{P}D \\ * & -cZ_1 & O & O & O & O \\ * & * & -cZ_1 & O & O & O \\ * & * & * & -cZ_2 & O & O \\ * & * & * & * & -c\hat{Z} & -cZ_1D \\ * & * & * & * & * & -\sigma I_n \end{bmatrix} < 0 \tag{42}$$

where * denotes the symmetric terms in a symmetric matrix. The relative matrices $\hat{\Psi}, A_{ci}, \hat{Z}, D, \hat{P}$ can be seen in the Appendix IV. The proof of Theorem 2 can be seen in [35] for detail.

V. SIMULATION STUDIES

To verify the correctness and effectiveness of the proposed method, in this paper, an integrated micro-grid system model consisting of five PDGs is built in Matlab/Simulink, as shown in Fig.4. The cost parameters are listed in Table II and the system operation parameters are listed in Table III. The load demands are scheduled as follows: in the interval [2s,8s], y_{load2} is connected to the microgrid, and y_{load3} is connected to the microgrid in the interval [4s,6s]. The test system is assumed that the ratings of all DGs is greater than demands.

The proposed method in this paper can realize the global optimal ED considering capacity constraint with high voltage recovery and robustness such as plug-and-play and load change. Moreover, the proposed method is stable and effective under delay and noise.

TABLE II
ECONOMICAL PARAMETERS OF PDGs

PDG$_i$	γ_i	β_i	α_i
1	1.06	5.00	2.00
2	0.86	0.12	4.00
3	1.75	4.00	4.00
4	2.50	3.00	2.00
5	1.00	6.00	5.00

TABLE III
THE SIMULINK PARAMETERS OF THE DC MICRO-GRID

Item	Symbol
Output filter inductor	$L_1 \sim L_5 = 0.60mH$
Output filter capacitor	$C_1 \sim C_5 = 95\mu F$
Reference voltage of PDG	$u_{ref} = 220V$
Virtual resistance	$r_{vir} = 0.1\Omega$
Line impedance	$y_1 = 2s, y_2 = 2.5s, y_3 = 1.67s$ $y_4 = 2s, y_5 = 1.43s$
Load impedance	$y_{load1} = y_{load2} = y_{load3} = (5/242)\, s$

Case 1, case 2 and case 8 are designed to verify the global optimal ED. Case 3 and case 4 are designed to verify the robustness of the proposed method. Case 3 and case 4 are designed to verify the robustness of the proposed method. Case 5 and case 6 are designed to verify the stability and effectiveness under delay and noise. Case 7 is designed to compare with peer technologies. The simulation results are as follows.

Case 1 (Consider capacity constraint of PDG$_i(i > 1)$): In this case, only consider the case where the output power of PDG$_i(i > 1)$ is limited and $p_2^{\max} = 500$W, $p_4^{\max} = 300$W. The output power among PDGs are depicted in Fig.5(a), in which PDG$_2$ keeps its maximum output power 500W in the interval [2s,8s] and PDG$_4$ keeps its maximum output power 300W in the interval [4s, 6s]. The voltage of DC is shown in Fig.5(c), where the bus voltage is maintained at around 220V. The equal increase rate of each PDG is shown in Fig.5(b). In the steady-state, except for those PDGs whose

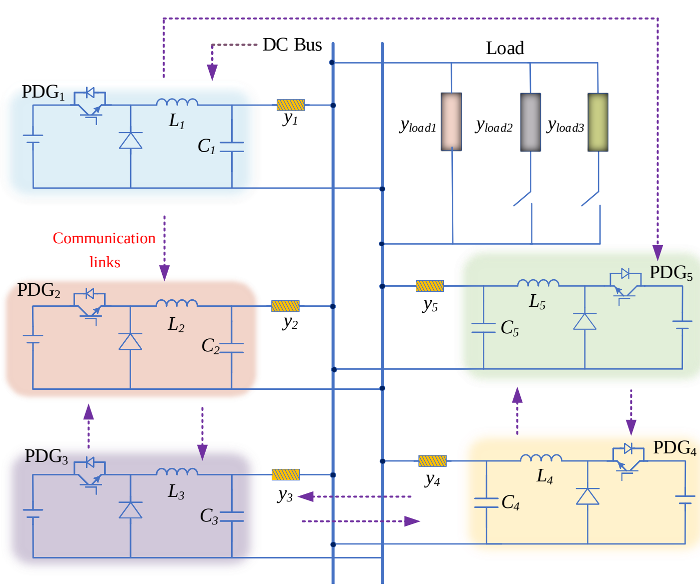

Fig. 4. The structure of the DC microgrid

This article has been accepted for publication in a future issue of this journal, but has not been fully edited. Content may change prior to final publication. Citation information: DOI 10.1109/JETCAS.2021.3049788, IEEE Journal on Emerging and Selected Topics in Circuits and Systems

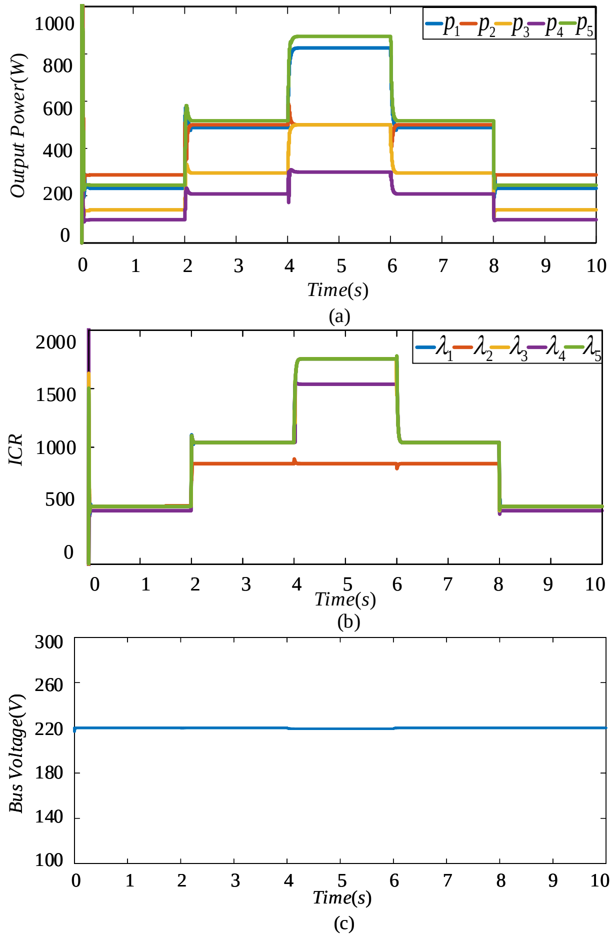

Fig. 5. Simulation results of case 1. (a) Output power, (b) Equal increase rate, (c) Bus voltage

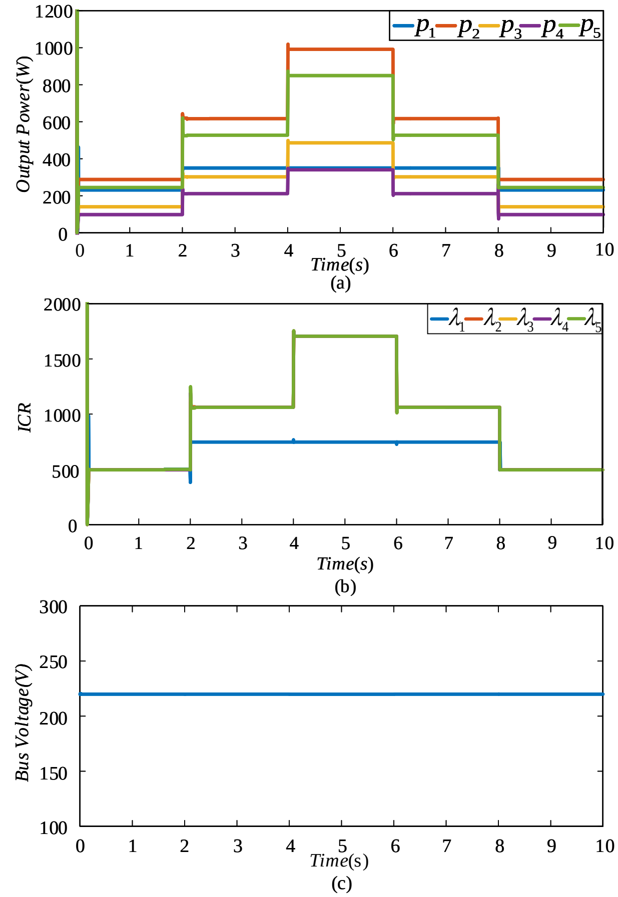

Fig. 6. Simulation results of case 2. (a) Output power, (b) Equal increase rate, (c) Bus voltage

output powers are maximum, other ICRs can reach the same value, which shows the global optimal ED considering the capacity constraint of PDG$_i(i > 1)$ can be achieved.

Case 2 (Consider the power limitation of PDG$_1$): In this case, only the capacity constraint of PDG$_1$ will be analyzed and $p_1^{\max} = 450$W. The corresponding simulation results are illustrated in Fig.6. It shows that the system stabilizes rapidly after PDG$_1$ is restricted in the interval [2s, 8s] and has a fast response to load change. The voltage of DC bus is shown in Fig.6(c). When PDG$_1$ reaches the restricted state and switches the control strategy, the bus voltage can still be restored to around the rated voltage and other ICRs can reach the same value, which shows the global optimal ED considering the capacity constraint of PDG$_i(i = 1)$ can be achieved and the accuracy of voltage recovery is high.

Case 3 (Simulation with plug-and-play): In this case, the system is tested via unplugging the PDG$_5$ at 1s and plugging PDG$_5$ back at 3s, and only $p_4^{\max} = 300$W is considered. The simulation results are shown in Fig.7. When PDG$_5$ is unplugged, the system quickly reaches a new steady state and other PDGs coordinate to make sure system economically optimal.Therefore, the proposed method can achieve plug-and-play.

Case 4 (Simulation with RDG and PDG): In this case, suppose the PDG$_5$ is RDG, which is controlled in the MPPT mode. Meanwhile $p_2^{\max} = 500$W and $p_4^{\max} = 300$W are considered. The simulation results are shown in Fig.8. Because the output power of RDG is time-varying, PDG$_2$ switches the control strategy accordingly. The result in case 4 shows the proposed method is effective and robust when the RGs and load change.

Case 5 (Simulation considering communication delay): After the communication delay had been considered, the performance of PDG was analysed in this case where the delay, $d(t)$, has been considered. Compared to Fig.5(a), it takes longer for the power to converge with the same k_u, k_λ considering the effect of communication delay shown in Fig.9(a). As the value of parameters k_u, k_λ increase from 1 to 2, the system will lose stability shown in Fig.9(b). This indicates that the propose method can be implemented with a certain delay and the design of parameters can be solved by solving linear matrix inequality in (42).

Case 6 (Robustness performance under noises): To test the robustness performances of proposed control, noise disturbances in communication links are taken into consideration in this case. Apparently, even though high-frequency noise exists in communication links, the system can still be stable shown in Fig.10. It verifies that the proposed control method also achieves economical dispatch and meets capacity constraint.

This article has been accepted for publication in a future issue of this journal, but has not been fully edited. Content may change prior to final publication. Citation information: DOI 10.1109/JETCAS.2021.3049788, IEEE Journal on Emerging and Selected Topics in Circuits and Systems

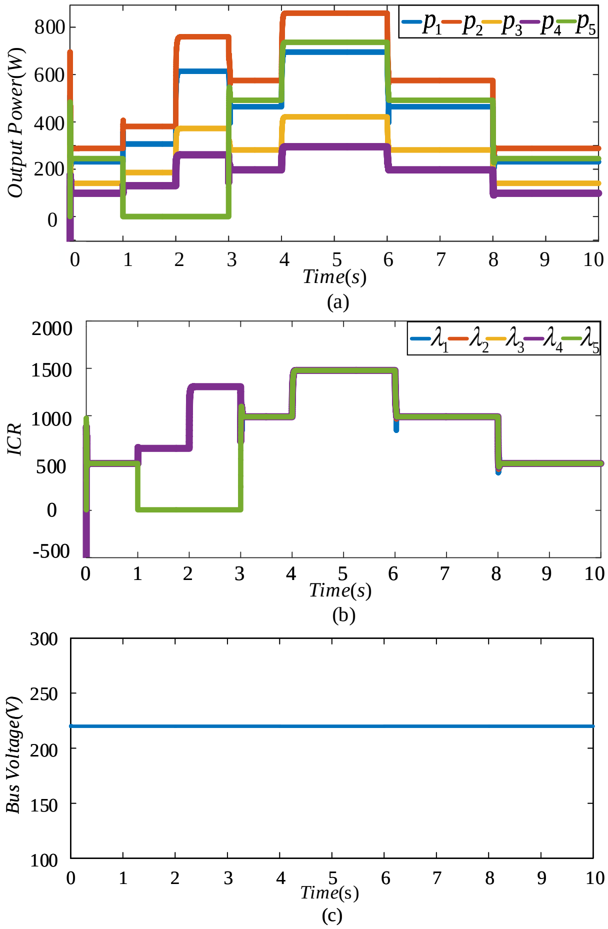

Fig. 7. Simulation results of case 3. (a) Output power, (b) Equal increase rate, (c) Bus voltage

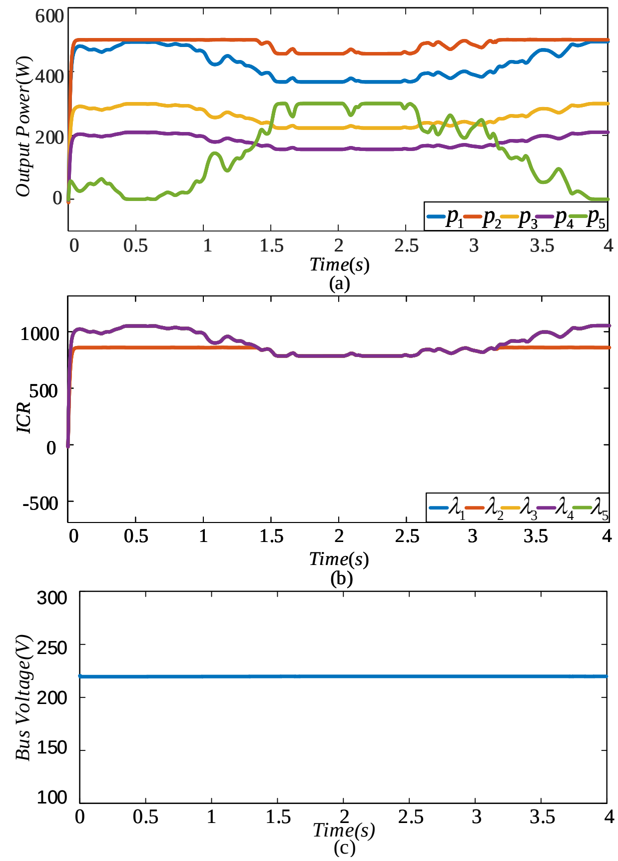

Fig. 8. Simulation results of case 4. (a) Output power, (b) Equal increase rate, (c) Bus voltage

Obviously, the proposed method is not sensitive to high-frequency noises.

Case 7 (Comparison with "virtual ICR" method and average voltage recovery): The performance of the proposed control scheme is compared with "virtual ICR" method [27]-[30] and average voltage recovery [25] [31]. We perform the simulation scenario of case 1 by exploiting the "virtual ICR", and present the results in Fig.11(a). Compare with Fig.5(b), the λ can not converge to the same as (5) for the reason that λ is calculated by output power in dynamic consensus, and the restricted λ should not continue to participate in subsequent calculations like the discrete consensus algorithm. Therefore, "virtual ICR" method can't receive global optimal ED in dynamic consensus control. In addition, Fig.11(b) shows the the performance difference of our proposed method and average voltage recovery. The line impedance is large than case 1 to widen the difference in this case. It is obvious that the bus voltage accuracy is lower than our proposed method.

Case 8 (Simulation in large system with heavy load) Eventually, to verify the effectiveness of the proposed method in larger system with heavy load, a system with ten PDGs and 60kW load demand is designed where $p_2^{\max} = 9$kW. The load changes from 50kW to 60kW at $t = 2s$, which is shown in Fig.12. The PDG$_2$ is controlled at the maximum power

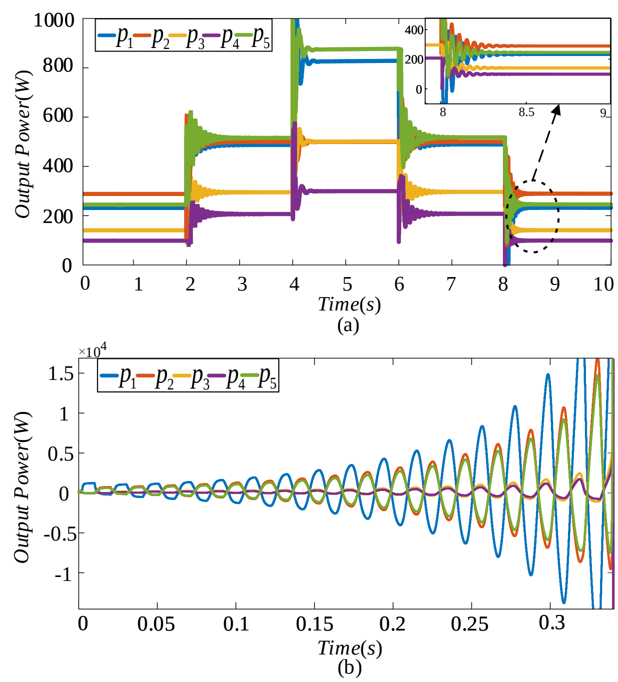

Fig. 9. Simulation results of case 5. (a) Output power with $k_u = 1$, $k_\lambda = 1$, d=50ms. (b) Output power with $k_u = 2$, $k_\lambda = 2$, d=50ms.

This article has been accepted for publication in a future issue of this journal, but has not been fully edited. Content may change prior to final publication. Citation information: DOI 10.1109/JETCAS.2021.3049788, IEEE Journal on Emerging and Selected Topics in Circuits and Systems

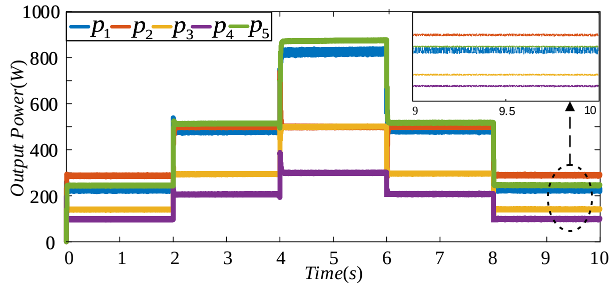

Fig. 10. Simulation results of case 6 with high-frequency noise

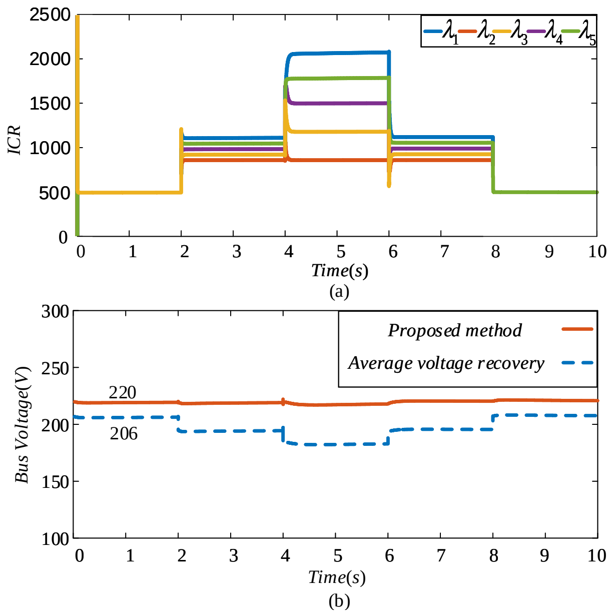

Fig. 11. Simulation results of case 7. (a) Performance of "virtual ICR" method in dynamic consensus, (b) Comparison of average voltage recovery

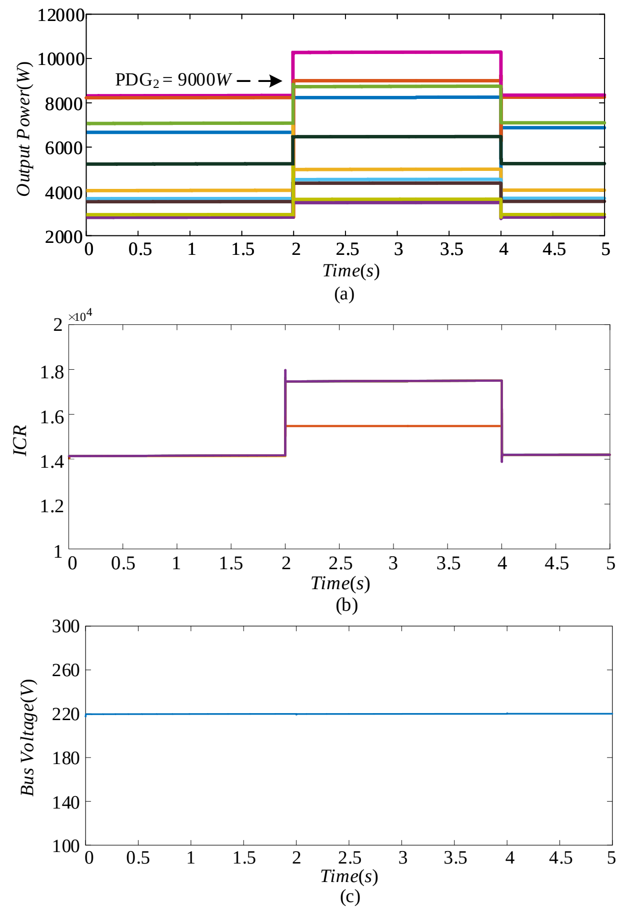

Fig. 12. Simulation results of case 8. (a) Output power, (b) Equal increase rate, (c) Bus voltage

when it reach capacity constraint in Fig.12(a) and others' ICR can reach the same in Fig.12(b), which indicates that the global optimal ED can be achieved. The global optimal ED is still achieved when more PDGs and larger load demand are considered in the system.

As a result, the proposed method can receive global optimal solution of ED with the consideration of capacity constraint, which can be seen in case 1, case 2 and case 8. Case 3 verifies the plug-and-play performance of proposed method. Case 4 shows that the proposed strategy is effective and robust with power fluctuation of RDG. Besides, the proposed method can resist certain communication delay and noise disturbances shown as case 5 and case 6. Compared with "virtual ICR", the proposed method can effectively solve the capacity constraint in dynamic consensus and receives higher voltage accuracy than average voltage recovery, which is illustrated in case 7.

VI. CONCLUSIONS

In this paper, a fully distributed optimal control strategy is presented to solve ED for islanded DC microgrids. Based on the proposed ED strategy, PDGs whose output power reach their capacity bounds are controlled to operate in a constant power mode, other PDGs share load in a distributed coordinate mode based on lambda consensus algorithm, and the smoothing switch of two control modes is triggered adaptively by its capacity bounds. The economic dispatch considering capacity constraint and the bus voltage recovery are achieved only depending on a sparse communication topology. Besides, the small-signal stability and steady convergence for the system is investigated by theoretical analysis and simulation experiment. Simulation results under communication delay, communication noise, communication fault, DG plug-in and plug-out show that the system exhibits good dynamic, static, stable, play-and-plug and robust performances.

REFERENCES

[1] L. Li, Y. Sun, H. Han, G. Shi, M. Su and M. Zheng, "A Decentralized Control for Cascaded Inverters in Grid-Connected Applications," *IEEE Trans. Ind. Electron.*, vol. 67, no. 9, pp. 8064-8071, Sept. 2020.

[2] Zhangjie Liu, Mei Su, Yao Sun, Hua Han, Xiaochao Hou, and Josep M. Guerrero, "Stability analysis of DC microgrids with constant power load under distributed control methods," *Automatica*, vol. 90, pp. 62-72, Apr. 2018.

[3] Sheetal Chandak, Pritam Bhowmik, Pravat Kumar Rout, " Load shedding strategy coordinated with storage device and D-STATCOM to enhance the microgrid stability," *Protection and Control of Modern Power Systems*, vol. 4, no. 3, pp. 250-269, Nov. 2019.

[4] J. Lai, X. Lu, X. Yu, W. Yao, J. Wen, and S. Cheng, "Distributed mult-DER cooperative control for master–slave-organized microgrid networks with limited communication bandwidth," *IEEE Trans. Ind. Informat.*, vol. 15, no. 6, pp. 3443–3456, Jun. 2019.

This article has been accepted for publication in a future issue of this journal, but has not been fully edited. Content may change prior to final publication. Citation information: DOI 10.1109/JETCAS.2021.3049788, IEEE Journal on Emerging and Selected Topics in Circuits and Systems

[5] Y. Sun, L. Li, G. Shi, X. Hou and M. Su, "Power Factor Angle Droop Control A General Decentralized Control of Cascaded Inverters," *IEEE Trans. Power Delivery*. doi: 10.1109/TPWRD.2020.3009842.

[6] X. Sun, B. Liu, Y. Cai, H. Zhang, Y. Zhu and B. Wang, "Frequency-based power management for photovoltaic/battery/fuel cell-electrolyser stand-alone microgrid," *IET Power Electronics*, vol. 9, no. 13, pp. 2602-2610, Oct. 2016.

[7] C. E. Lin and G. L. Viviani, "Hierarchical Economic Dispatch for Piecewise Quadratic Cost Functions," *IEEE Trans. Power Appar. Syst.*, vol. PAS-103, no. 6, pp. 1170-1175, Jun. 1984.

[8] V. V. S. N. Murty and Ashwani Kumar, "Multi-objective energy management in microgrids with hybrid energy sources and battery energy storage systems." *Protection and Control of Modern Power Systems*, vol. 5, no. 1, Jan. 2020. doi: 10.1186/s41601-019-0147-z

[9] Mehdi Farokhian Firuzi, Alireza Roosta, Mohsen Gitizadeh, "Stability analysis and decentralized control of inverter-based ac microgrid," *Protection and Control of Modern Power Systems*, vol. 4, no. 1, Mar. 2019. doi: 10.1186/s41601-019-0120-x

[10] Yao Sun, Guangze Shi, Xing Li, Wenbin Yuan, Mei Su, Hua Han, Xiaochao Hou, "An f-P/Q Droop Control in Cascaded-type Microgrid," *IEEE Transactions on Power Systems*, vol. 33, no. 1, pp. 1136-1138, Jan. 2018.

[11] A. Bidram and A. Davoudi, "Hierarchical Structure of Microgrids Control System," *IEEE Trans. Smart Grid*, vol. 3, no. 4, pp. 1963-1976, Dec. 2012.

[12] J. M. Guerrero, J. C. Vasquez, J. Matas, L. G. de Vicuna and M. Castilla, "Hierarchical Control of Droop-Controlled AC and DC Microgrids—A General Approach Toward Standardization," *IEEE Trans. Ind. Electron.*, vol. 58, no. 1, pp. 158-172, Jan. 2011.

[13] J. Sun, V. Palade, X. Wu, W. Fang and Z. Wang, "Solving the Power Economic Dispatch Problem With Generator Constraints by Random Drift Particle Swarm Optimization," *IEEE Trans. Ind. Informat.*, vol. 10, no. 1, pp. 222-232, Feb. 2014.

[14] Po-Hung Chen and Hong-Chan Chang, "Large-scale economic dispatch by genetic algorithm," *IEEE Transactions on Power Systems*, vol. 10, no. 4, pp. 1919-1926, Nov. 1995.

[15] M. H. Sulaiman, H. Daniyal and M. W. Mustafa, "Modified Firefly Algorithm in solving economic dispatch problems with practical constraints," *2012 IEEE International Conference on Power and Energy (PECon), Kota Kinabalu*, 2012, pp. 157-161.

[16] G. s. s. Babu, D. b. Das and C. Patvardhan, "Real-parameter quantum evolutionary algorithm for economic load dispatch," *IET Gener. Transm. Distrib.*, vol. 2, no. 1, pp. 22-31, Jan. 2008.

[17] Y. Zhu and H. Gao, "Improved Binary Artificial Fish Swarm Algorithm and Fast Constraint Processing for Large Scale Unit Commitment," *IEEE Access*, vol. 8, pp. 152081-152092, Aug. 2020.

[18] J. Lai, X. Lu, X. Yu, A. Monti and H. Zhou, "Distributed Voltage Regulation for Cyber-Physical Microgrids With Coupling Delays and Slow Switching Topologies," *IEEE Trans. Syst., Man, Cybern., Syst.*, vol. 50, no. 1, pp. 100-110, Jan. 2020.

[19] Baghaee H R, Mirsalim M, Gharehpetian G B, et al. "A Generalized Descriptor-System Robust H∞ Control of Autonomous Microgrids to Improve Small and Large Signal Stability Considering Communication Delays and Load Nonlinearities," *International Journal of Electrical Power & Energy Systems*, vol. 92, pp. 63-82, Nov. 2017.

[20] J. Lai, X. Lu, X. Yu and A. Monti, "Stochastic Distributed Secondary Control for AC Microgrids via Event-Triggered Communication," *IEEE Trans. Smart Grid*, vol. 11, no. 4, pp. 2746-2759, Jul. 2020.

[21] J. Lai and X. Lu, "Nonlinear Mean-Square Power Sharing Control for AC Microgrids Under Distributed Event Detection," *IEEE Trans. Ind. Informat.*, vol. 17, no. 1, pp. 219-229, Jan. 2021.

[22] V. Nasirian, F. L. Lewis and A. Davoudi, "Distributed optimal dispatch for DC distribution networks," *2015 IEEE First International Conference on DC Microgrids (ICDCM), Atlanta, GA*, pp. 97-101, 2015.

[23] I. U. Nutkani, W. Peng, P. C. Loh and F. Blaabjerg, "Cost-based droop scheme for DC microgrid," *2014 IEEE Energy Conversion Congress and Exposition (ECCE), Pittsburgh, PA*, pp. 765-769, 2014.

[24] J. Hu, J. Duan, H. Ma and M. Chow, "Distributed Adaptive Droop Control for Optimal Power Dispatch in DC Microgrid," *IEEE Trans. Ind. Electron.*, vol. 65, no. 1, pp. 778-789, Jan. 2018.

[25] H. Han, H. Wang, Y. Sun, J. Yang, Z.Liu, "Distributed control scheme on cost optimisation under communication delays for DC microgrids," *IET Gener. Transm. Distrib.*, vol. 11, no. 17. pp. 4193-4201, Jul. 2017.

[26] Yi P, Hong Y, Liu F, "Initialization-free Distributed Algorithms for Optimal Resource Allocation with Feasibility Constraints and its Application to Economic Dispatch of Power Systems," *Automatica*, vol. 74, no. 259-269, Dec. 2016.

[27] R. Wang, Q. Li, B. Zhang and L. Wang, "Distributed Consensus Based Algorithm for Economic Dispatch in a Microgrid," *IEEE Trans. Smart Grid*, vol. 10, no. 4, pp. 3630-3640, Jul. 2019.

[28] Q. Li, D. W. Gao, H. Zhang, Z. Wu and F. Wang, "Consensus-Based Distributed Economic Dispatch Control Method in Power Systems," *IEEE Trans. Smart Grid*, vol. 10, no. 1, pp. 941-954, Jan. 2019.

[29] Z. Wang, W. Wu, and B. Zhang, "A fully distributed power dispatch method for fast frequency recovery and minimal generation cost in autonomous microgrids," *IEEE Trans. Smart Grid*, vol. 7, no. 1, pp. 19–31, Jan. 2016.

[30] S. Yang, S. Tan, and J. Xu, "Consensus based approach for economic dispatch problem in a smart grid," *IEEE Trans. Power Syst.*, vol. 28, no. 4, pp. 4416–4426, Nov. 2013.

[31] Z. Liu, M. Su, Y. Liu, H. Wang and H. Han, "A distributed control scheme with cost optimization and capacity constraints," *IECON 2017 - 43rd Annual Conference of the IEEE Industrial Electronics Society*, Beijing, 2017, pp. 521-526.

[32] Z. Wang, W. Wu and B. Zhang, "A Distributed Control Method With Minimum Generation Cost for DC Microgrids," *IEEE Trans. Energy Convers.*, vol. 31, no. 4, pp. 1462-1470, Dec. 2016.

[33] C. Li, X. Yu and W. Yu, Optimal economic dispatch by fast distributed gradient: *2014 13th International Conference on Control Automation Robotics & Vision (ICARCV)*, Singapore, 2014, pp. 571-576.

[34] S. Yang, S. Tan and J. Xu, "Consensus Based Approach for Economic Dispatch Problem in a Smart Grid," *IEEE Trans. Power Syst.*, vol. 28, no. 4, pp. 4416-4426, Nov. 2013.

[35] Y. He, Q. Wang, L. Xie and C. Lin, "Further Improvement of Free-Weighting Matrices Technique for Systems With Time-Varying Delay," *IEEE Trans. Autom. Control*, vol. 52, no. 2, pp. 293-299, Feb. 2007.

Appendix

Appendix I

Theorem 1: If L is a balanced Laplacian matrix and $K = diag\{k_i\}$ has positive diagonal elements, b is a constant coefficient, then, $L' = bLKL$ is a symmetric positive semi-definite matrix, which has only one zero eigenvalue and $\ker(L') = 1_n$.

Proof: Because matrix L is a Laplacian matrix of a strongly connected undirected graph, then $1^T L = 0$. $L' = bLKL$ then $L' = bLK(L1_n) = 0$. On the other hand, $1_n^T L' = b\left(1_n^T L\right) KL = 0$, which shows $\ker(L') = 1_n$.

Appendix II

The L_{ss},L_{sl},L_{ls},L_{ll} in the admittance matrix Y are as follows, $L_{ss} = diag\{y_i\}$, $L_{ll} = \sum_{i=1}^{n} y_i$,
$L_{sl} = [-y_1 \cdots - y_n]^T, L_{ls} = [-y_1 \cdots - y_n]$

Appendix III

The parameter matrices in (38) are given as follows,

$$A_{d1} = (I_n + r_{vir}Y_0)^{-1}T$$
$$\Delta A_{d1} \approx \frac{\Delta y_{load}(I_n + r_{vir}Y_0)^{-1}}{(y_{load}+L_{ll})^2}(A_1 + A_2 - L_{sl}(I_n + r_{vir}Y_0)^{-1}T)$$

where matrices A_1, A_2 are as follows,

$$A_1 = k_u \tau L_{ls}, A_2 = k_\lambda (I_n - \tau\tau^T) L\gamma diag\{u_i^{ss}\} L_{sl}$$

The parameter matrices in (40) are given as follows,

$$A_{b2} = \begin{bmatrix} A_3 & 0 \\ 0 & C_1 \end{bmatrix}, A_{d2} = \begin{bmatrix} A_4 & B_1 \\ 0 & 0 \end{bmatrix}$$
$$\Delta A_{b2} \approx \Delta y_{load}(t) \begin{bmatrix} A_5 & 0 \\ 0 & C_2 \end{bmatrix}$$
$$\Delta A_{d2} \approx \Delta y_{load}(t) \begin{bmatrix} A_6 & B_2 \\ 0 & 0 \end{bmatrix}$$

This article has been accepted for publication in a future issue of this journal, but has not been fully edited. Content may change prior to final publication. Citation information: DOI 10.1109/JETCAS.2021.3049788, IEEE Journal on Emerging and Selected Topics in Circuits and Systems

where related matrices are as follows,

$$
\begin{aligned}
&A_3 = -k_p(I_n + r_{vir}Y_0)^{-1}\tau\Phi \\
&A_4 = -k_\lambda(I_n + r_{vir}Y_0)^{-1}(I_n - \tau\tau^T)L\gamma\Phi \\
&B_1 = k_u k_\lambda(I_n + r_{vir}Y_0)^{-1}(I_n - \tau\tau^T)L\tau \\
&C_1 = -(y_{load} + L_{ll})^{-1}L_{sl} \\
&A_5 = \tfrac{k_p(I_n+r_{vir}Y_0)^{-1}}{(y_{load}+L_{ll})^2}(A_{51} + A_{52}) \\
&A_{51} = \tau diag\{u_i^{ss}\}L_{sl}L_{ls} \\
&A_{52} = r_{vir}L_{sl}L_{ls}(I_n + r_{vir}Y_0)^{-1}\tau\Phi \\
&A_6 == \tfrac{k_\lambda(I_n+r_{vir}Y_0)^{-1}}{(y_{load}+L_{ll})^2}(A_{61} + A_{62}) \\
&A_{61} = L_{sl}L_{ls}(I_n + r_{vir}Y_0)^{-1}(I_n - \tau\tau^T)L\gamma\Phi \\
&A_{62} = (I_n - \tau\tau^T)L\gamma diag\{u_i^{ss}\}L_{sl}L_{ls} \\
&B_2 = \tfrac{-k_u k_\lambda r_{vir}}{(y_{load}+L_{ll})^2}B_{21} \\
&B_{21} = (I_n + r_{vir}Y_0)^{-1}L_{sl}L_{ls}(I_n - \tau\tau^T)L\tau \\
&C_2 = -\tfrac{L_{sl}}{(y_{load}+L_{ll})^2}
\end{aligned}
$$

The parameter matrices in (41) are given as follows,

$$
\begin{aligned}
&E_{d1} = \tfrac{\xi(I_n+r_{vir}Y_0)^{-1}}{(y_{load}+L_{ll})^2}(A_1 + A_2 - L_{sl}(I_n + r_{vir}Y_0)^{-1}T) \\
&E_{d1} = \xi\begin{bmatrix} A_5 & 0 \\ 0 & C_2 \end{bmatrix}, E_{d2} = \xi\begin{bmatrix} A_6 & B_2 \\ 0 & 0 \end{bmatrix}
\end{aligned}
$$

Appendix IV

The parameter matrices in (43) are given as follows

$$
\begin{aligned}
&\hat{\Psi} = \Psi + \begin{bmatrix} \sigma E_{bi}^T E_{bi} & \sigma E_{bi}^T E_{di} & \mathrm{O} \\ * & \sigma E_{di}^T E_{di} & \mathrm{O} \\ * & * & \mathrm{O} \end{bmatrix}, \hat{P} = \begin{bmatrix} P \\ \mathrm{O} \\ \mathrm{O} \end{bmatrix} \\
&\Psi = \Psi_1 + \Psi_2 + \Psi_2^T, \hat{Z} = Z_1 + Z_2 \\
&\Psi_1 = \begin{bmatrix} PA_{bi} + A_{bi}^T P + Q + R & PA_{di} & \mathrm{O} \\ * & -(1-\mu)Q & \mathrm{O} \\ * & * & -R \end{bmatrix} \\
&\Psi_2 = \begin{bmatrix} N + M & -N + S & -M - S \end{bmatrix} \\
&A_{ci} = \begin{bmatrix} A_{bi} & A_{di} & \mathrm{O} \end{bmatrix}
\end{aligned}
$$

where $i = 1, 2$ and $E_{b1} = \mathrm{O}$.

Hua Han received the M.S. and Ph.D. degrees from the School of Automation, Central South University, Changsha, China, in 1998 and 2008, respectively. She was a Visiting Scholar with the University of Central Florida, Orlando, FL, USA, from 2011 to 2012. She is currently a Professor with the School of Automation, Central South University.

Her research interests include microgrids, renewable energy power generation systems, and power electronic equipment.

Xinyu Chen received the B.S. degree in electrical engineering, in 2019, from Central South University,Changsha, Hunan, China, where he is currently working toward the M.S. degree in electrical engineering.

His research interests include distributed control, economic dispatch and Renewable Energy Systems.

Zhangjie Liu received the B.S. degree, in 2013, in Detection Guidance and Control Techniques and the Ph. D. degree in Control Science and Engineering from the Central South University, Changsha, China. He is currently an Associate Professor at School of Automation of Central South University. He is also a Postdoctoral Research Fellow at the Nanyang Technological University.

He is interested in DC microgrid, power system stability, complex network and nonlinear circuit.

Yonglu Liu was born in Chongqing, China, in 1989. He received the B.S., M.S., and Ph.D. degrees in electrical engineering from Central South University, Changsha, China, in 2012, 2015, and 2017 respectively. He has been an Associate Professor with School of Automation, Central South University, China.

His research interests include power electronics and renewable energy power conversion systems.

Mei Su received the B.S., M.S., and Ph.D. degrees from the School of Information Science and Engineering, Central South University, Changsha, China, in 1989, 1992, and 2005, respectively. Since 2006, she has been a Professor with the School of Information Science and Engineering, Central South University.

Her research interests include matrix converter, adjustable speed drives, and wind energy conversion system.

Shimiao Chen received the B.S. degree in electrical engineering, in 2019, from Central South University, Changsha, Hunan, China. From 2019, he is currently working toward the M.S. degree in power electronics with the College of Automation.

His research interests include renewable energy, power electronic transient stability analysis, and control of converters.